Molecular Mobility of the Ca^{2+}-Deficient EF-Hand of Cardiac Troponin C As Revealed by Fluorescence Polarization of Genetically Inserted Tryptophan[†]

Venu G. Rao, Arvind B. Akella, Hong Su, and Jagdish Gulati*

The Molecular Physiology Laboratory, Division of Cardiology, Departments of Medicine and Physiology/Biophysics, Albert Einstein College of Medicine, 1300 Morris Park Avenue, Bronx, New York 10461

Received July 11, 1994; Revised Manuscript Received October 18, 1994[®]

ABSTRACT: To probe attitudinal features of the Ca^{2+}-deficient site (site I) in the Ca^{2+} switch of cardiac troponin C (cTnC), we have examined steady-state fluorescence emission and polarization of a Trp26 inserted in a recombinant cardiac TnC (cTnC3.W) and compared these with the properties of the Ca^{2+}-competent site I in skeletal TnC (sTnC4.W). The Ca^{2+}-induced fluorescence emission in cTnC3.W was a fraction (25–30%) of that in sTnC4.W, in agreement with previous observations on the Ca^{2+}-deficient site incorporated in a cardiac/skeletal chimera c1/s.W [Gulati, J. & Rao, V. G. (1994) *Biochemistry 33*, 9052–9056]. Thus, the fractional quantum yield reflected intrinsic properties of the cardiac metal ion-deficient site I. Conversely, in sTnC-1.W, where the skeletal site I also was made Ca^{2+}-deficient by D^{27}→A substitution, the Ca^{2+}-induced quantum yield was lower than that in cTnC3.W. Nevertheless, similar steady-state fluorescence polarizations for Ca^{2+}-saturated sTnC4.W and cTnC3.W indicated indistinguishable final conformations in the two activated TnC isoforms. In EGTA, the polarization parameter (P_{EGTA}) of sTnC4.W is greater than that of cardiac TnC, and the cardiac P_{EGTA} value is closer to the activated P_{Ca}. Comparison of the chimera c1/s.W with sTnC-1.W indicated that the differences in conformation of the site I Trp for the EGTA-treated cardiac/skeletal isoforms were due to the structural disparities in this region. This contention was further supported by examination of the chimera CBc1/s.W, where the cardiac EF-hand was altered by ^{27}VLGA^{30}→DAD substitution. Polarization of the relaxed form was similar to that for sTnC4.W. These findings suggest that the relaxed conformation of the cardiac Ca^{2+} switch is more favorably predisposed to activation than the skeletal switch.

The contractilities in cardiac and skeletal muscles are triggered by Ca^{2+} binding to the respective troponin C's (TnC's),[1] but the underlying molecular events in the switching mechanisms, especially those in cardiac muscle, remain unclear. Skeletal TnC (sTnC) is a dumbbell-shaped molecule with two Ca^{2+}-binding EF-hand structures in each of the N- and C-terminal lobes (Strynadka & James, 1989), but muscle activation is correlated with Ca^{2+} binding to the N-terminal sites (sites I and II, putative trigger sites) (Sheng et al., 1990; Babu et al., 1992; Gulati et al., 1993). Cardiac TnC (cTnC) also contains four EF-hands, but differs from skeletal TnC in that Ca^{2+} binds only site II of the trigger site pair (Van Eerd & Takahashi, 1976; Leavis & Kraft, 1978). Nonetheless, the Ca^{2+}-deficient cardiac site I maintains an essential role in the activation switching mechanism. The study of cardiac/skeletal chimeras in cardiotrabeculae indicates that residues 1–41 (containing site I) of cardiac TnC are necessary to elicit cardiac contractility (Gulati et al., 1992). The goal was to explore the molecular alterations in the Ca^{2+}-deficient site to further define its role in the activation of cardiac contractility.

Recent insights into the mechanistic aspects of the cardiac Ca^{2+} switch for contractile activation were inferred from steady-state fluorescence emissions by the excited tryptophan (Trp26) in the Ca^{2+}-deficient region (site I) of a modified cardiac/skeletal chimera (Gulati & Rao, 1994). The quantum yield of the tryptophan was enhanced in saturating Ca^{2+}, suggesting that the site I region was active when the switch was turned on. However, the Ca^{2+}-induced increment in quantum yield in the chimera was a mere fraction (approximately 25%) of that recorded in skeletal TnC. It was unclear whether this difference during activation reflected modified conformational changes directly in the fluorophore vicinity, or whether the Ca^{2+}-induced alterations elsewhere in the molecule generated microenvironmental influences that varied between the cardiac and skeletal tryptophans. To investigate these possibilities, we have expanded the study to include fluorescence measurements with polarized light.

We also studied the cardiac site I EF-hand of cTnC to address the possibility that the observed Ca^{2+}-dependent fractional increment in quantum yield in the cTnC/sTnC chimera might be specific to this chimeric construct. Additional concern that the quenched fluorescence response of the tryptophan in cardiac EF-hand might result simply from the failure of cardiac site I to bind Ca^{2+} was also explored, with a mutated rabbit skeletal TnC in which site I was

---

[†] Grant support was from the NIH (AR 33736) and the New York Heart Association. Part of the equipment was purchased with support from the Blumkin Fund.

[®] Abstract published in *Advance ACS Abstracts*, December 15, 1994.

[1] Abbreviations: TnC, troponin C; cTnC, bovine cardiac TnC; sTnC, rabbit skeletal fast-twitch muscle troponin C; PCR, polymerase chain reaction; MOPS, 4-morpholinopropanesulfonic acid; PAGE, polyacrylamide gel electrophoresis; EGTA, [ethylenebis(oxyethylenenitrilo)]-tetraacetic acid; DTT, dithiothreitol; IPTG, isopropyl β-thiogalactopyronaside; DAN, dansyl; DDP, 4-(dimethylamino)-3,5-dinitrophenyl; SEM, standard error of the mean; *F*, the measured peak of the fluorescence emission; *P*, polarization.

0006-2960/95/0434-562$09.00/0

disabled, substituting a noncoordinating residue for Asp27 in the *x*-coordinate of the EF-hand loop (Babu et al., 1992).

Both the steady-state fluorescence quantum yields and polarizations were compared between the tryptophan derivatives of the various proteins. The quantum yields of cTnC in EGTA and Ca^{2+} confirmed the findings on the Ca^{2+}-deficient EF-hand in the paradigmatic chimera. Moreover, the fluorescence polarizations, by recording Ca^{2+}-dependent modifications in segmental conformations and/or flexibilities under well-defined conditions (Cantor & Shimmel, 1980), suggested a more favorable contractile predisposition for the cardiac EF-hand than that of its skeletal counterpart, which is a surprising finding. The possible impacts of these on the switching mechanism for cardiac contractile activation are also noted.

MATERIALS AND METHODS

All chemicals were of high grade and were purchased from Sigma, unless otherwise mentioned. The radiolabeled $^{45}Ca^{2+}$ was purchased from Amersham. Reagent-grade water (specific resistivity > 17.5 MΩ) was used throughout the experiments. The $CaCl_2$ stock solution was from Orion Company.

1. Mutagenesis. The various protein constructs used in the present study are depicted in Figure 1 for clarity. The Trp derivatives of both the wild-type and mutant proteins are shown. By convention, the recombinant sTnC and cTnC are called sTnC4 and cTnC3, respectively, to distinguish them from tissue proteins.

Both the normal and tryptophan 26 derivatives of skeletal TnC (sTnC4 and sTnC4.W), the cardiac/skeletal chimera with Ca^{2+}-deficient site I (c1/s and c1/s.W), and the Ca^{2+}-binding variants (CBc1/s and CBc1/s.W) were the same as before (Gulati & Rao, 1994). The tryptophan derivative of sTnC-1, an inactive skeletal TnC in which site I was made Ca^{2+}-deficient by replacing the putative *x*-coordinate in the skeletal EF-hand [see Kretsinger (1980)] from Asp^{27}→Ala, was generated especially for this study. The rationale was based on previous work indicating that x-coordinate Asp was critical for Ca^{2+} binding in the generic EF-hand (Babu et al., 1992). The Ca^{2+} binding was rechecked (see the following).

2. Synthesis of a cTnC cDNA. The cDNA coding for bovine cardiac TnC was engendered from a series of oligomeric cassettes, as described for sTnC (Babu et al., 1992), except that only 15 restriction sites were possible in the present instance (Figure 2). The cDNA was inserted into a pT7 plasmid, which employs the T7 RNA polymerase for directing the expression of the cloned gene. The codon for tryptophan was inserted in position 26 by replacing that for phenylalanine, exactly as in the other constructs. Because no tryptophan existed in bovine cTnC or rabbit sTnC, Trp26 provided a ready spectroscopic marker that could be followed with ease (Gulati & Rao, 1994). The nucleotide sequences of the mutants were verified by DNA sequencing.

The proteins were expressed in *Escherichia coli* (DE3-pLysS cells, Novagen) under the specific induction of IPTG. The purification of the bacterially synthesized proteins was carried out by column chromatography as described previously [Babu et al., 1992; see also Xu and Hitchcock-DeGregori (1989)]. Each protein was checked by SDS–PAGE, which indicated a single band with a characteristic Ca^{2+} dependency (Gulati et al., 1992).

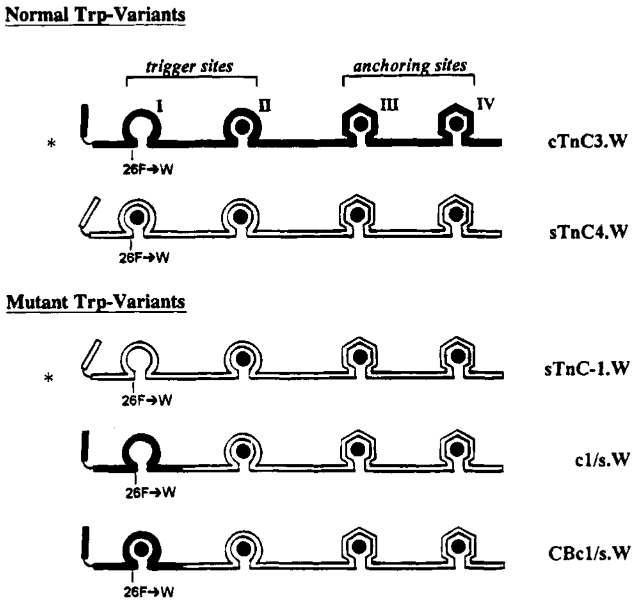

FIGURE 1: Diagrammatic representation of the Trp variants of the various proteins used in this study. The cTnC3.W and sTnC-1.W marked by stars are the two new proteins. The roman numerals I and II are the Ca-specific sites, and III and IV are the Ca/Mg sites. The black circles within the loops indicate Ca occupancy.

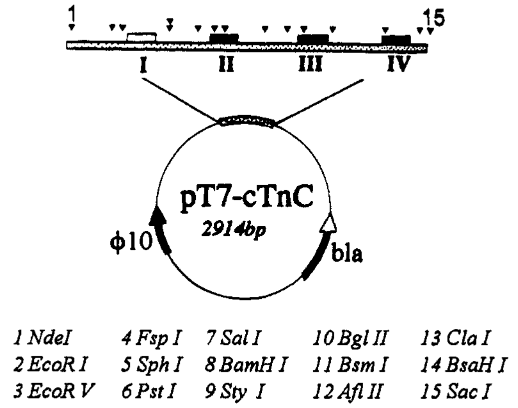

FIGURE 2: Physical map of the plasmid pT7-cTnC. The cTnC gene was synthesized with 15 restriction sites. The numbers I, II, III, and IV denote the Ca^{2+}-deficient (open) and Ca^{2+}-binding loops (black).

3. $^{45}Ca^{2+}$-Binding Potentials. These measurements were made on both the normal and Trp derivatives of recombinant cTnC3 and on sTnC-1. The saturating Ca^{2+} values were determined at pCa 3.5 by equilibrium microdialysis, as before (Gulati et al., 1992). Both sTnC4 and sTnC4.W were included as controls.

4. Far-UV Circular Dichroism. The far-UV CD spectra between wavelengths 215 and 250 nm were measured at 25 °C, using a Jasco J720 spectropolarimeter. The measurements were made in 50 mM KCl, 2 mM HEPES (pH 7.0), 1 mM DTT, and 2 mM EDTA or 3 mM $CaCl_2$. The protein concentration was 0.2 mg/mL, and the quartz cuvette path length was 1 mm. From the measured CD, the ellipticities (θ) were estimated at 222 nm (Greenfield & Fasman, 1969). The percentage α-helicities were computed (Lux et al., 1972) as follows: $\%\ \alpha\text{-helix} = ((-[\theta_{222}] + 3000)/39000) \times 100$.

5. Intrinsic Fluorescence Emissions and Steady-State Polarizations. Tryptophan fluorescence emission spectra were recorded between 300 and 400 nm on a Shimadzu RF5000U spectrofluorophotometer as before (Gulati & Rao, 1994). The excitation and emission spectra were collected at 5 nm bandpass resolution using a 295 nm wavelength for Trp excitation. The protein concentration for these experiments was 0.1 mg/mL. The cuvette (1 cm path length) was maintained at 25 °C, and the solution was stirred continuously.

All spectral measurements were performed in 100 mM MOPS (pH 7.0), 100 mM KCl, 1 mM EGTA, and 10 mM DTT at 25 °C. The buffer was treated with Chelex resin as described previously (Gulati & Rao, 1994) to remove the metal ion impurities. The results are expressed throughout as means ± SEM.

The fluorescence polarizations were also measured with the Shimadzu spectrofluorophotometer, but the instrument was additionally equipped with Shimadzu polarization accessory lenses. The experimental conditions were similar to those described earlier for the measurements of fluorescence emissions. The excitation wavelength was set to 295 nm to avoid the effects of energy transfer from tyrosines on the polarization parameter. The polarization measurements were made possible by studying the excitations and emissions with the polarized light beam oriented alternately in the parallel and perpendicular modes. The peak-polarized emission spectra were measured in the range 342−345 nm. The polarization values were estimated by the following equation (Chen & Bowman, 1965):

$$P = (I_{\mathrm{VV}} - GI_{\mathrm{VH}})/(I_{\mathrm{VV}} + GI_{\mathrm{VH}})$$

where, I_{VV} is the fluorescence intensity with both excitation and emission vertical, I_{VH} is the fluorescence intensity with excitation vertical and emission horizontal, and G is the grating correction factor ($=I_{\mathrm{HV}}/I_{\mathrm{HH}}$). The polarization ($P$) and anisotropy ($r$) can be interchanged using the equation $r = 2P/(3 - P)$.

In the absence of alterations in rotational diffusion or energy transfer, the changes in polarization (P) values reflect the degree of freedom of the fluorophore. The P value can achieve a theoretical maximum of 0.5 and a minimum of −0.33; the maximum would correspond to a rigid fluorophore, and the minimum would represent the angular displacement of 90° between the absorption and emission dipoles of the fluorophore [Lakowicz, 1983 (p 120)].

RESULTS

1. Ca^{2+} Binding and Far-UV Circular Dichroism of the Designed Trp Variants of cTnC and sTnC-1. A primary aim of the present study was to elucidate the activation mechanism in cardiac TnC. We approached this by systematic measurements of steady-state fluorescence polarizations of a genetically inserted tryptophan 26 in cardiac and skeletal TnC's (Figure 1). The cardiac EF-hand was examined in both cTnC3.W and the chimera c1/s.W (each with Trp26). In addition, we recorded the fluorescence signals from a mutant sTnC-1.W to ascertain whether the present cardiac properties were the direct effects of Ca^{2+} deficiency or whether these were true structural manifestations of the cardiac isoform. This aspect was also explored with the CBc1/s.W chimera, in which the Ca^{2+} deficiency had been amended by the replacement of the cardiac ^{27}VLGA^{30} cluster with skeletal DAD (Gulati & Rao, 1994).

Table 1: Maximal $^{45}Ca^{2+}$ Binding to Purified Proteins in pCa 3.5 Solution[a]

normal variants		tryptophan variants	
protein	bound Ca^{2+} (mol/mol)	protein	bound Ca^{2+} (mol/mol)
sTnC4	3.81 ± 0.1	sTnC4.W	4.16 ± 0.1
cTnC3	2.53 ± 0.1	cTnC3.W	2.57 ± 0.1
sTnC-1	3.10 ± 0.1	sTnC-1.W	3.17 ± 0.1

[a] In each case, the data are the means of six experiments.

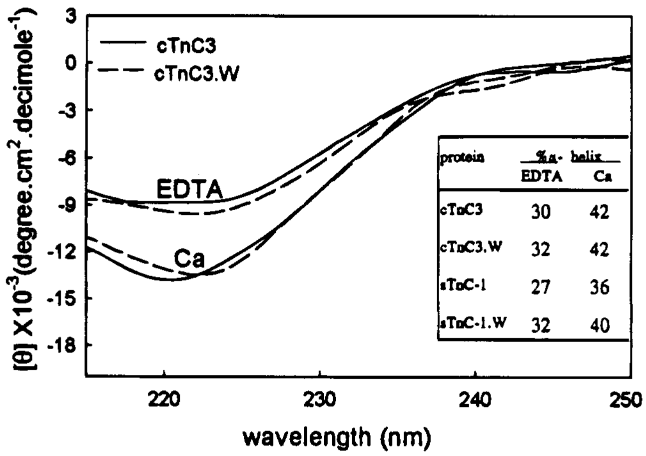

FIGURE 3: Far-UV CD spectra of cardiac TnC and the Trp derivative of the protein. The upper spectra are in the presence of 2 mM EDTA and the bottom spectra are in the presence of 3 mM $CaCl_2$. The protein concentration was 0.2 mg/mL. The inset table shows % α-helicity of the various proteins.

To verify the functional integrity of the new recombinant proteins cTnC3.W and sTnC-1.W, we measured their Ca^{2+}-binding capacities. As a further check on the structure, circular dichroism spectra of normal and tryptophan-containing variants were compared as well.

1.1. $^{45}Ca^{2+}$ Binding. The Ca^{2+}-binding capacities of cTnC3, sTnC-1, and their Trp derivatives were measured at pCa 3.5 and are listed in Table 1 in comparison with sTnC4. The Ca^{2+} binding in these proteins was unaffected by the insertion of tryptophan for phenylalanine 26. The Ca^{2+}-binding capacities in c1/s, CBc1/s, and their Trp derivatives were measured previously and had the expected values (c1/s and c1/s.W, 3 Ca^{2+} bound mol/mol; CBc1/s and CBc1/s.W, close to 4 Ca^{2+} bound mol/mol; Gulati & Rao, 1994).

1.2. Far-UV CD Characteristics. Typical CD spectra of cTnC3 and cTnC3.W in the absence and presence of Ca^{2+} are shown in Figure 3. The overall similarity in these spectra rules out the possibility of a disruptive influence of Trp 26 on these proteins [see also Pearlstone et al. (1992)]. Similar results were obtained for sTnC-1 and sTnC-1.W (not shown). The ellipticity (θ) for the various proteins was estimated at 222 nm, and the α-helicities calculated from these values (see Materials and Methods) are listed in the inset to Figure 3. These comparisons provide additional confidence that any global disruptions due to the Trp replacement are immaterial to the overall function.

2. Fluorescence Spectral Properties of the Trp Variants. 2.1. Quantum Yields in cTnC3.W and the Cardiac/Skeletal Chimera c1/s.W. The emission spectra of Trp26 in cTnC3.W and c1/s.W were compared to determine the properties of the cardiac EF-hand in these different structural milieus. Typical results with and without Ca^{2+} are depicted in Figure 4A. The wild-type cTnC3.W and the chimera c1/s.W each

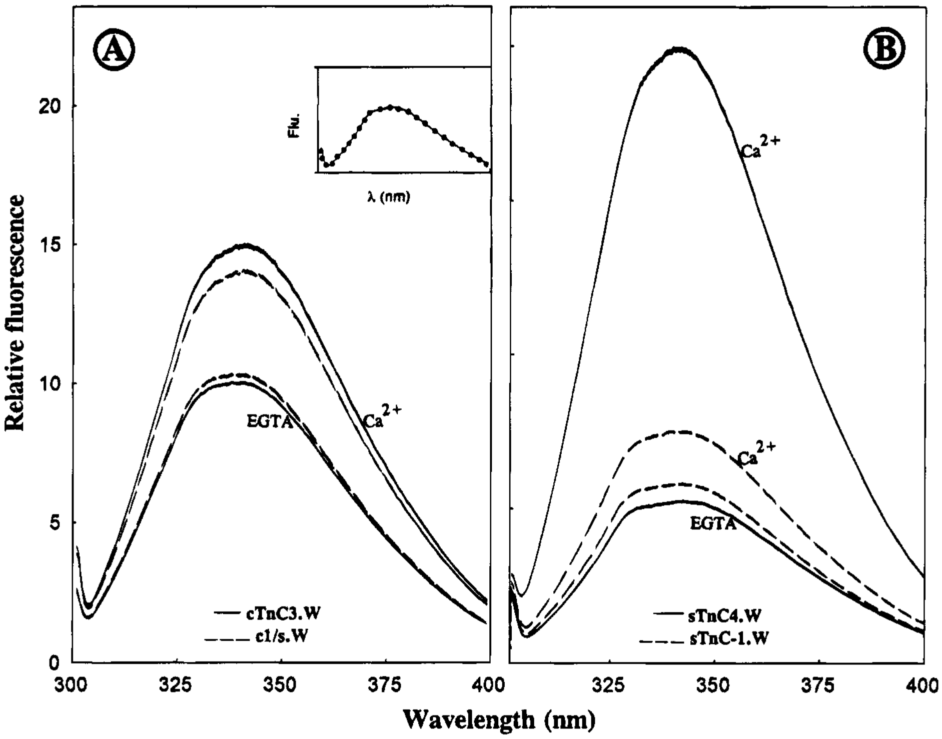

FIGURE 4: Relative fluorescence emission spectra of Ca^{2+}-free (bottom) and Ca^{2+}-bound (upper) forms of Trp variants. The spectra were recorded at an excitation wavelength of 295 nm. (A) Emission spectra of cTnC3.W (—) and cI/s.W (— —). The inset figure shows the fluorescence spectra of cTnC3.W in the absence (—) and the presence (●) of 9 mM MgCl$_2$. (B) Spectra of sTnC4.W (—) and sTnC-1.W (— —). The protein concentration was 0.1 mg/mL in all cases.

Table 2: Relative Quantum Yields of Tryptophan Variants in EGTA and pCa 4 Solution[a]

protein	relative quantum yield	
	EGTA	+Ca
cardiac variants		
cTnC3.W	1.00 ± 0.05	1.44 ± 0.03
cI/s.W	1.05 ± 0.07	1.40 ± 0.09
skeletal variants		
sTnC4.W	0.58 ± 0.05	2.10 ± 0.15
sTnC-1.W	0.64 ± 0.04	0.84 ± 0.05

[a] In each case, the data are the means of four experiments, and the means are normalized relative to cTnC3.W in EGTA.

showed increased emission intensity with saturating Ca^{2+} over EGTA. The peak wavelength was 338.7 ± 0.2 nm in EGTA and was slightly red-shifted to 340.1 ± 0.1 nm (n = 4) at pCa 4, in both proteins. The peak intensities in EGTA and at pCa 4, normalized to the peak emission by cTnC3.W in EGTA, are denoted as relative quantum yields in Table 2.

For cTnC3.W, the relative quantum yield in saturating Ca^{2+} was 1.44, compared with the normalized value of 1.00 in EGTA. The fluorescence emission had remained unaffected by the inclusion of 9 mM MgCl$_2$ in EGTA solution (see the inset to Figure 4A for a typical spectrum for cTnC3.W). The Ca/Mg sites III and IV (putative anchoring sites) would be saturated at the present level (8.75 mM) of free Mg; the complete absence of a Mg effect on fluorescence suggests that the increase in Trp26 response with saturating Ca^{2+} is due largely to metal ion binding to site II. Comparable changes to cTnC3.W with Ca^{2+} were observed on the chimera cI/s.W. The relative quantum yields of cI/s.W were 1.05 (normalized to cTnC3.W) in EGTA and 1.40 at pCa 4 (Table 2). This indicates that the cardiac EF-hand behaves similarly in both the cI/s.W and cTnC3.W constructs.

2.2. Trp26 Spectral Properties in sTnC4.W and sTnC-1.W. Figure 4B compares the emission spectra between sTnC-1.W and sTnC4.W in both EGTA and Ca^{2+} solutions. In EGTA, sTnC4.W and sTnC-1.W generated nearly similar fluorescence emissions (compare the lower two curves in Figure 4B). This further indicates that site I mutation in sTnC-1.W had left the global structure relatively intact.

We next compared the emission spectra with saturating Ca^{2+}. The steady-state fluorescence peak intensity increased, but the increment in sTnC-1.W was less than that in wild-type sTnC4.W (see Table 2). The maximal emission wavelengths for sTnC-1.W and sTnC4.W in EGTA were 341.0 ± 0.1 nm (n = 4) and 342.3 ± 0.1 nm (n = 8), respectively. Such a shift in the emission wavelengths is possible because of the polar to nonpolar residue conversion of D^{27} to A. With Ca^{2+}, the emission wavelength of sTnC-1.W was unaltered (341.0 nm), but that for sTnC4.W was blue-shifted by 2.6 nm to 339.7 nm. This blue shift is indicative that microenvironment of the Trp during Ca^{2+} activation becomes more hydrophobic and suggests that the Trp experiences a more nonpolar microenvironment, either due to the accompanying conformational shifts or due to Ca^{2+} binding to site I in sTnC4.W, but not in sTnC-1.W, excluding water in loop I from the vicinity of the fluorophore.

The peak quantum yields relative to cTnC3.W are noted in Table 2. The comparisons between sTnC-1.W and cI/s.W (also cTnC3.W), each containing one Ca^{2+}-deficient EF-hand and three Ca^{2+}-competent sites, indicate that the structural characteristics of cardiac EF-hand are distinct from those of the genetically manipulated Ca^{2+}-deficient site in sTnC-1.W. This will be further explored presently with fluorescence polarizations.

Table 3: Polarization Parameters in EGTA and pCa 4 Solution[a]

polarization (P)	sTnC4.W (i)	cTnC3.W (ii)	c1/s.W (iii)	CBc1/s.W (iv)	sTnC-1.W (v)
P_{EGTA}	0.166 ± 0.004	0.138 ± 0.002	0.137 ± 0.003	0.154 ± 0.002	0.171 ± 0.003
P_{Ca}	0.103 ± 0.001	0.106 ± 0.001	0.106 ± 0.003	0.104 ± 0.002	0.126 ± 0.002

[a] In each case, the data are the means ($N = 4$) of four experiments. P_{EGTA} and P_{Ca} were measured in 1 mM EGTA and pCa 4 solutions, respectively.

3. Steady-State Fluorescence Polarizations of Trp Variants of cTnC3 and sTnC4. The fluorescence polarization parameter was measured on various proteins in dilute buffer solutions (0.1−0.2 mg/mL) to deduce the structural underpinnings for the differences between cardiac and skeletal TnC functions. The polarization values were computed as described under Materials and Methods, and these measurements in EGTA and at pCa 4 are recorded in Table 3 for all proteins.

For sTnC4.W, the polarization value in EGTA (P_{EGTA}) was estimated as 0.166 and diminished at pCa 4 (P_{Ca}) to 0.103 (column i in Table 3; see also Table 3 in Cheung et al. (1991)). For cTnC3.W, Ca^{2+} saturation also diminished the P value to 0.106, which is indistinguishable from the corresponding value in sTnC4.W. This suggests that the conformations and/or flexibilities of site I between the Ca^{2+}-saturated sTnC4.W and cTnC3.W are similar. Interestingly, in the absence of Ca^{2+}, polarization for cTnC3.W was 0.136, which is significantly lower than the corresponding EGTA value in sTnC4.W. Evidently, the relaxed (EGTA) configuration of cardiac site I is highly predisposed toward the fully activated configuration, in comparison with the behavior of skeletal site I. A specific model incorporating this possibility will be discussed in the following. Because chimera c1/s.W also shows lower polarization in EGTA (column iii in Table 3), this behavior of cardiac site I is a characteristic manifestation of the intrinsic structure and not that of the overall milieu.

In CBc1/s.W, the Ca^{2+}-competent variant of the chimera, the EGTA polarization became similar to that of sTnC4.W (column iv in Table 3). Since in this construct the ^{27}VLGA^{30} polypeptide is genetically replaced by DAD (Gulati & Rao, 1994), the polarization measurements provide a strong demonstration that the four particular residues have a marked effect on the mobility of the EF-hand. In other words, by virtue of cardiac to skeletal alterations in four amino acid residues (VLGA, cardiac; DAD, skeletal), the CBc1/s.W chimera managed to achieve the skeletal-type polarization both in the EGTA (apo state) as well as in the Ca^{2+}-bound forms.

4. Polarizations in the sTnC-1.W Construct. We also measured the EGTA and Ca^{2+} polarizations in sTnC-1.W. In this construct, D^{27} had been converted to Ala [see also Babu et al. (1992)] to manifest Ca^{2+} dis-coordination in site I. The Trp26 polarization for the mutant in EGTA was found to be 0.171, which is close to the value in sTnC4.W. In pCa 4, the polarization (P_{Ca}) was 0.126, which is an intermediate value (column v in Table 3).

DISCUSSION

Toward efforts to understand the regulation of contractility in cardiac muscle, the present study sought specific insights into the molecular mobilities in the vicinity of the trigger domain of TnC. Like skeletal TnC, cardiac TnC also has four EF-hands (sites I and II in the N-terminal lobe and sites III and IV in the C-terminal lobe), but cardiac site I is Ca^{2+}-deficient (Van Eerd & Takahashi, 1976). Nonetheless, recent studies suggest that the Ca^{2+} deficiency, although required for the cardiac (Gulati et al., 1989, 1991) as well as the slow-muscle phenotypes (Sweeney et al., 1990), cannot fully explain the on−off mechanism of the cardiac switch. For instance, the c1/s chimera, in which the Ca^{2+}-deficient cardiac EF-hand (site I) was spliced with sites II−IV of skeletal TnC, maintained cardiac-type regulation. In contrast, sTnC-1, with skeletal site I rendered Ca^{2+}-deficient by mutation of the metal ion-coordinating residues, was unable to trigger myocardial contraction (Gulati et al., 1992). Notably, CBc1/s, in which cardiac site I had been made Ca^{2+}-competent by the replacement $^{27}\mathrm{VLGA}^{30}\rightarrow\mathrm{DAD}$, indicated the skeletal phenotype (Gulati & Rao, 1994). Evidently, the structure of cardiac site I engenders greater functional diversity than that permitted within the skeletal regulatory domain [see also Gulati & Rao (1994)]. The present findings on fluorescence polarization suggest a possible structural explanation (see Figure 5). We show here that the cardiac EF-hand in the relaxed state is in a relatively open configuration compared with the relaxed state of sTnC. The activated, fully open configurations in both the cardiac and skeletal isoforms are identical, however.

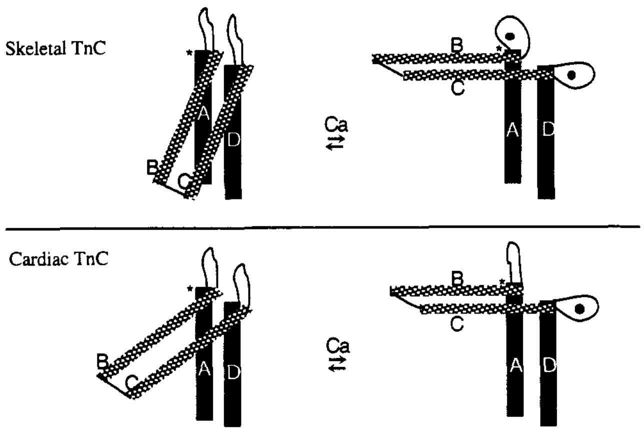

FIGURE 5: Proposed mechanism of the cardiac switch. Ca^{2+}-induced transitions in the N-terminal region of TnC are depicted. A, B and C, D are the α-helix pairs in the EF-hands of sites I and II, respectively. The off state is on the left and the on state is on the right. The cardiac off state is preinclined toward the activated form. The sketch for sTnC was modified from Gergely etal. (1993).

As noted previously (see introduction), the earlier indication of a Ca^{2+}-dependent conformational difference between sites I of the cardiac and skeletal regulatory domains had come from comparisons of steady-state fluorescence emissions of a genetically inserted tryptophan in sTnC4.W and c1/s.W (Gulati & Rao, 1994). For the cardiac EF-hand in the chimera, the maximal fluorescence intensity with saturating Ca^{2+} was a fraction of that in sTnC4.W. The present results with cTnC3.W are in agreement with those for c1/s.W and indicate that the activation mechanism of the cardiac EF-hand is similar in both the chimera and the wild-type cTnC3. Furthermore, interestingly, in the relaxed state the polarization measurements reveal that the conformation of the trigger region in cardiac TnC with the Ca^{2+}-deficient site is closer to that of the activated state compared with sTnC4.

Steady-state fluorescence polarization or anisotropy can provide direct information about flexibility or rigidity, but it requires knowledge of the fluorescence lifetime of the excited fluorophore (τ), as well as the rotational correlation time (ϕ). This can be illustrated by the simplified Perrin equation for anisotropy: $r = r_0/(1 + \tau/\phi)$, where r is the measured (steady-state) anisotropy and equals r_0, the intrinsic anisotropy (zero time), only for $\tau \ll \phi$. Judging from the polarization in EGTA, we find that the relaxed cardiac site I has lower P (and r) values compared with skeletal site I (Table 3). In the absence of direct time-resolved studies and anisotropy decays, thus, we cannot resolve whether these polarizations are due to modified flexibilities of the trigger sites or whether variant lifetimes and correlation times are responsible. However, for either situation, the cardiac/skeletal differences in polarizations (and anisotropies) in EGTA and their confluence in the Ca^{2+}-saturated states can be interpreted most simply to indicate that final Ca^{2+}-activated conformational states are similar in the two isoforms. Interestingly, since the relaxed polarization value in cardiac TnC was closer to the activated polarization value, this also suggests that a defining feature of the cardiac switch is the evident ease by which the transition is made to the on-state (see below). This may be useful for the optimal systolic–diastolic heart beat and might also be important in governing the cardiac response to variable physiological demands on the organism.

The findings on sTnC-1.W yielded further insights into the mechanism of the cardiac switch. Although the EGTA conformation of this mutant is similar to that of sTnC4.W, the results in the activated state in solution are striking in that they indicate that the mutant failed to achieve the final open conformation observed in other proteins (i.e., c1/s and cTnC). The sTnC-1 mutant was also ineffective in switching on cardiac muscle contractility with Ca^{2+} (Gulati et al., 1992). This supports the possibility of a correlation between the final polarization value in saturating Ca^{2+} for the protein and whether or not it will remain functional. This is also additional evidence that the cardiac structure of the Ca-deficient trigger site is well-adapted to function and that metal ion deficiency itself accounts for only a part of the adaptation.

Mechanism of the Cardiac Ca^{2+} Switch. The crystal structure of turkey sTnC has suggested a specific model for the Ca^{2+} switch (Herzberg et al., 1986). In this scheme, upon binding Ca^{2+}, sites I and II unfold from their resting closed configuration in EGTA into the open configuration. Moreover, these rearrangements are coupled with the bending of helices B and C relative to helices A and D (Figure 5). A number of recent studies have provided experimental support for this model for sTnC. For instance, Wang et al. (1992) labeled a genetically inserted Cys12 (in A-helix) and Cys49 (in B-helix) with DAN and DDP, respectively, and using the fluorescence resonance energy transfer (FRET) technique, they measured the separation distances of 28 and 39 Å in the apo and Ca^{2+}-saturated states, respectively, in rabbit sTnC. The observed 11 Å enhancement was close to the change predicted in Herzberg et al. (1986). Similarly, Grabarek et al. (1990) showed that the TnC switch was inoperative when the Ca^{2+}-induced separations of the B- and C-helices from the central helix were prevented by disulfide bonds in another double-Cys (Cys48, Cys82) construct.

Since cTnC is also a 4-EF-hand protein, the corresponding cardiac mechanism too might be extrapolated from sTnC. One such possibility is included in Figure 5. Because the polarization parameter for cTnC3.W in EGTA was closer to its final value at pCa 4 than was the case for sTnC4.W (Table 3), it could be argued that the cardiac B- and C-helices (in EGTA) are already inclined toward the open (pCa 4) state. Presumably, therefore, the cardiac switch is highly mobile and excitable even while turned off. The lower quantum yield for cTnC3.W than for sTnC4.W examined in the open state suggests that during the unfolding of the switch the Ca^{2+}-deficient loop may remain constrained relative to the loop in skeletal site I (Figure 5). As the loop opens in sTnC, it affects the nearby Trp and produces a characteristic increase in quantum yield. In the cardiac switch, the Trp remains exposed throughout. An alternative explanation for the differences in the Ca^{2+} dependencies of quantum yields and polarizations between sTnC4.W and cTnC3.W could be that Ca^{2+} binding in sTnC releases the observed Phe26–Met45 linkage (Herzberg et al., 1986) and affects the fluorophore. Presumably, this mechanism differs in cTnC. These ideas deserve to be investigated in the future.

ACKNOWLEDGMENT

We thank the staff of the Laboratory of Macromolecular Analysis and the Oligonucleotide Synthesis Facility (both at the Albert Einstein College of Medicine) for help with circular dichroism measurements and with the oligomers.

REFERENCES

Babu, A., Su. H., Ryu, Y., & Gulati, J. (1992) *J. Biol.Chem. 267*, 15469–15474.

Cantor, C. R., & Shimmel, P. R. (1980) *Biophysical Chemistry*, Part II, W. H. Freeman & Co., New York.

Chen, R. F., & Bowman, R. L (1965) *Science 147*, 729–732.

Cheung, H. C., Wang, C., Gryczynski, I., Wiczak, W., Laczko, G., Johnson, M. L., & Lakowicz, J. R. (1991) *Biochemistry 30*, 5238–5247.

Gergely, J., Grabarek, Z., & Tao, T. (1993) in *Guidebook to the Cytoskeletal and Motor Proteins* (Kreis, T., & Vale, R., Eds.) pp 87–89, Oxford University Press, New York.

Grabarek, Z., Tan, R. Y., Wang, J., Tao, T., & Gergely, J. (1990) *Nature 345*, 132–135.

Greenfield, N., & Fasman, G. D. (1969) *Biochemistry 8*, 4108–4116.

Gulati, J., & Rao, V. G. (1994) *Biochemistry 33*, 9052–9056.

Gulati, J., Babu, A., & Putkey, J. (1989) *FEBS Lett. 248*, 5–8.

Gulati, J., Sonnenblick, E., & Babu, A. (1991) *J. Physiol. 441*, 305–324.

Gulati, J., Babu, A., & Su, H. (1992) *J. Biol. Chem. 267*, 25073–25077.

Gulati, J., Babu, A., Cheng, R., & Su, H. (1993) in *Modulation of Cardiac Calcium Sensitivity: a New Approch to Increasing the Strength of the Heart* (Lee, J. A., & Allen, D. G., Eds.) pp 215–241, Oxford University Press, New York.

Herzberg, M. N. G., Moult, J., & James, M. N. G. (1986) *J. Biol. Chem. 261*, 2638–2644.

Kretsinger, R. H. (1980) *CRC Crit. Rev. Biochem. 8*, 119–174.

Lakowicz, J. R. (1983) *Principles of Fluorescence Spectroscopy*, Plenum Press, New York.

Leavis, P. C., & Kraft, E. L. (1978) *Arch. Biochem. Biophys. 186*, 411–415.

Leavis, P. C., & Gergely, J. (1984) *Crit. Rev. Biochem. Mol. Biol. 16*, 235–305.

Lux, S. E., Hirz, R., Shrager, R. I., & Gotto, A. M. (1972) *J. Biol. Chem. 247*, 2598–2606.

Pearlstone, J. R., Borgford, T., Chandra, M., Oikawa, K., Kay, C. M., Herzberg, O., Moult J., Herklotz, A., Reinach, F., & Smillie, L. B. (1992) *Biochemistry 31*, 6545–6553.

Sheng, Z., Strauss, W. L., Francois, J.-M., & Potter, J. D. (1990) *J. Biol. Chem. 265*, 21554–21560.

Strynadka, N. C. J., & James, M. N. G. (1989) *Annu. Rev. Biochem. 58*, 951–998.

Sweeney, H. L., Brito, R., Rosevear, P. R., & Putkey, J. (1990) *Proc. Natl. Acad. Sci. U.S.A. 87*, 9538–9542.

Van Eerd, P. C., & Takahashi, K. (1976) *Biochemistry 15*, 1171–1180.

Wang, Z., Gergely, J., & Tao, T. (1992) *Proc. Natl. Acad. Sci. U.S.A. 89*, 11814–11817.

Xu, G.-Q., & Hitchcock-DeGregori, S. E (1988) *J. Biol. Chem. 258*, 9175–9177.

BI9415356